1998 Yampi Shelf, Browse Basin Airborne Laser Fluorosensor Survey Interpretation Report [WGC Yampi Survey]

Prepared For
Australian Geological Survey Organisation

April 2000

AGSO Record No. 2000/30

Prepared by: Robert Cowley
Signalworks Pty Ltd
A.C.N. 066 681 598
Email: rob.cowley@explorationist.com
WWW: http://www.explorationist.com/
Date: April 2000

Australian Geological Survey Organisation

Chief Executive Officer: Neil Williams

Department of Industry, Science & Resources

Minister for Industry, Science & Resources: Senator The Hon. Nick Minchin
Parliamentary Secretary: The Hon. Warren Entsch, MP

ISSN: 1039-0073
ISBN: 0 642 39847 X

Bibliographic reference: Cowley, R., 2000. 1998 Yampi Shelf, Browse Basin Airborne Laser Fluorosensor Survey Interpretation Report. Australian Geological Survey Organisation, Record 2000/30.

Contents

1. Introduction

The Yampi airborne laser fluorosensor (ALF) survey is located in the Yampi Shelf, Browse Basin (Figure 1). The survey was flown in several flights and sorties in November 1998. Sixty nine lines were acquired at 700m spacing in a NW-SE direction at a flying height of 80m. Line lengths ranged from 14.7km to 74.6km, with a total of 3,148.4km acquired.

A total of 2,149,037 spectra were collected at an average spacing of 1.38m to 2.13m. Of these 37 were selected as confident fluorescence spectra in the initial interpretation (17 fluors per million spectra). 132 fluorescence spectra were picked on the second more detailed interpretation (61 fluors per million spectra).

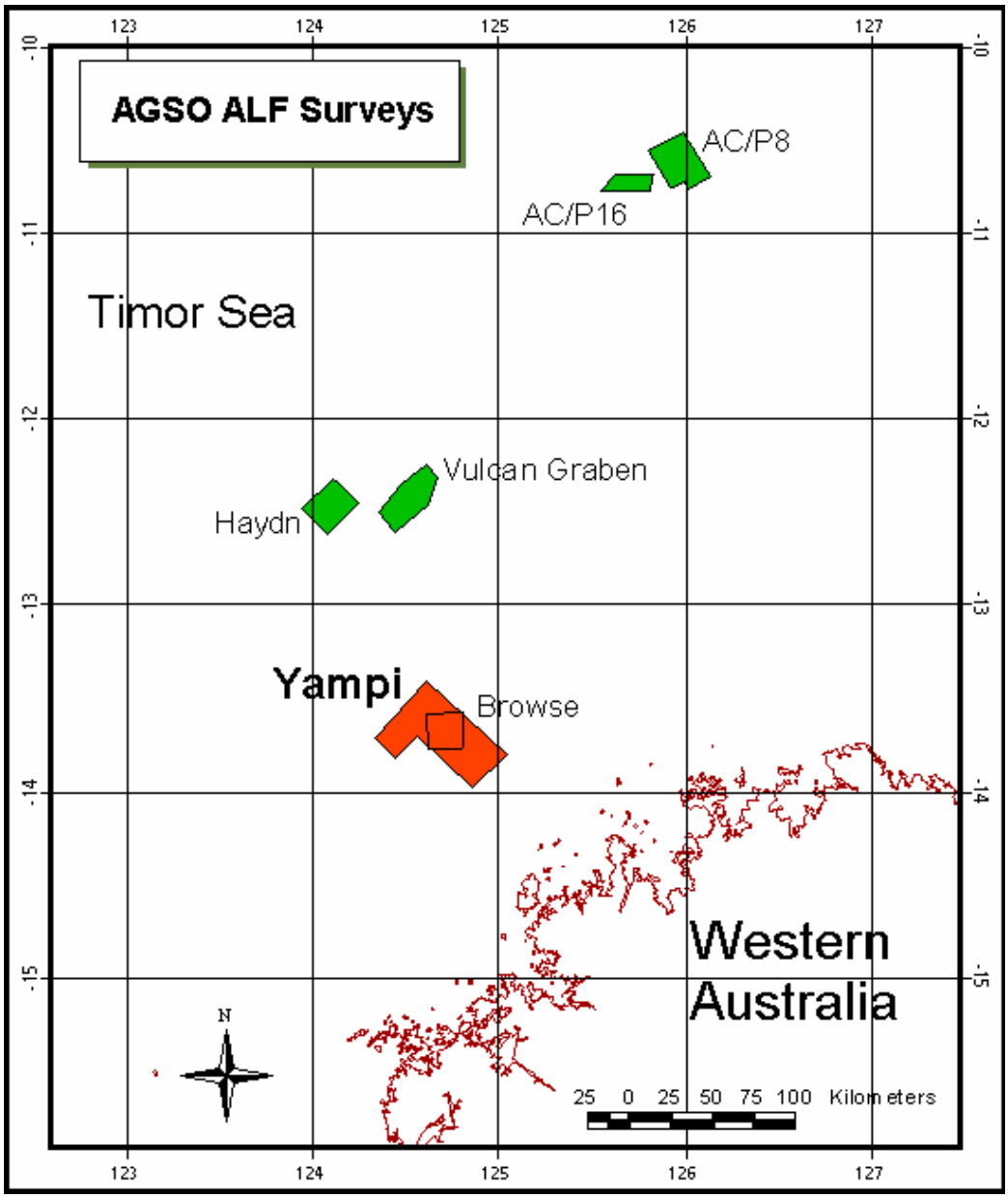

Figure 1. Yampi ALF Survey Location Map.

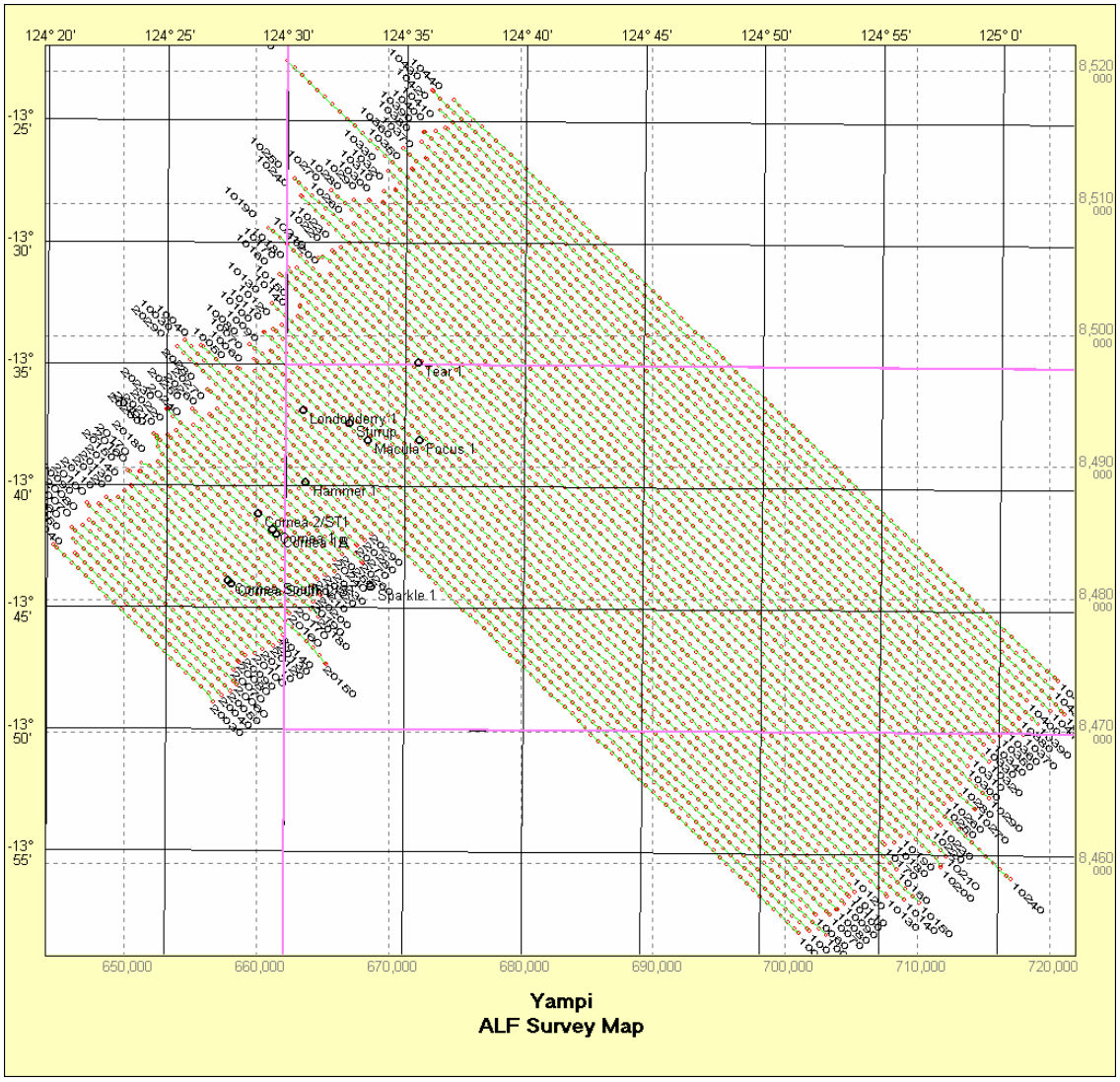

Figure 2. The Yampi ALF Survey.

Figure 2 shows a map of the Yampi ALF survey with point symbols annotated in red at a spacing of 500. The survey is located mainly in permit WA-266-P but also extends into permits WA-265-P, WA-241-P and WA98-7.

The extension of short lines covering the Cornea wells was flown as a separate survey. This survey repeated the line numbers used in the earlier survey so the first digit in each line was changed from “1” to “2” so both surveys could be combined in the one project.

Mapping Specifications:
Projection: Southern UTM Zone 51 (Central Meridian 123 degrees east)
Min Easting: 644,000
Max Easting: 722,000
Min Northing: 8,453,000
Max Northing: 8,522,000

This data interpretation project was undertaken for the Australian Geological Survey Organisation (AGSO) with interpretation requirements and technical advice provided by AGSO representatives Dianne Edwards and Mike Morse.

Several enhancements were made to the ALF Tools software to produce the required analyses including:

- Adjacent fluor detection module
- ASCII output of fluor data
- Fluor size histogram plotting
- Laboratory spectra import
- Laboratory spectra matching module.

2. ALF Survey Analysis

2.1. First Pass Fluor Mapping

A first pass fluorescence anomaly mapping was done using a channel 50 cutoff amplitude of 1000 to reduce the number of spectra to review from 2,149,037 to 1,731 possible fluors, then manually selecting the confident fluors. The following SQL query is used to select the possible fluors:

SELECT * FROM [RawAlfData] WHERE Ch_50 > 1000 ORDER BY Ch_50 DESC

Of the 1,731 possible fluors, 37 were picked as confident fluors and plotted in Figure 3. Each fluor is plotted as a red circle with size proportional to the fluorescence area / Raman area ratio. The most obvious and confident fluors tend to plot with the largest circles.

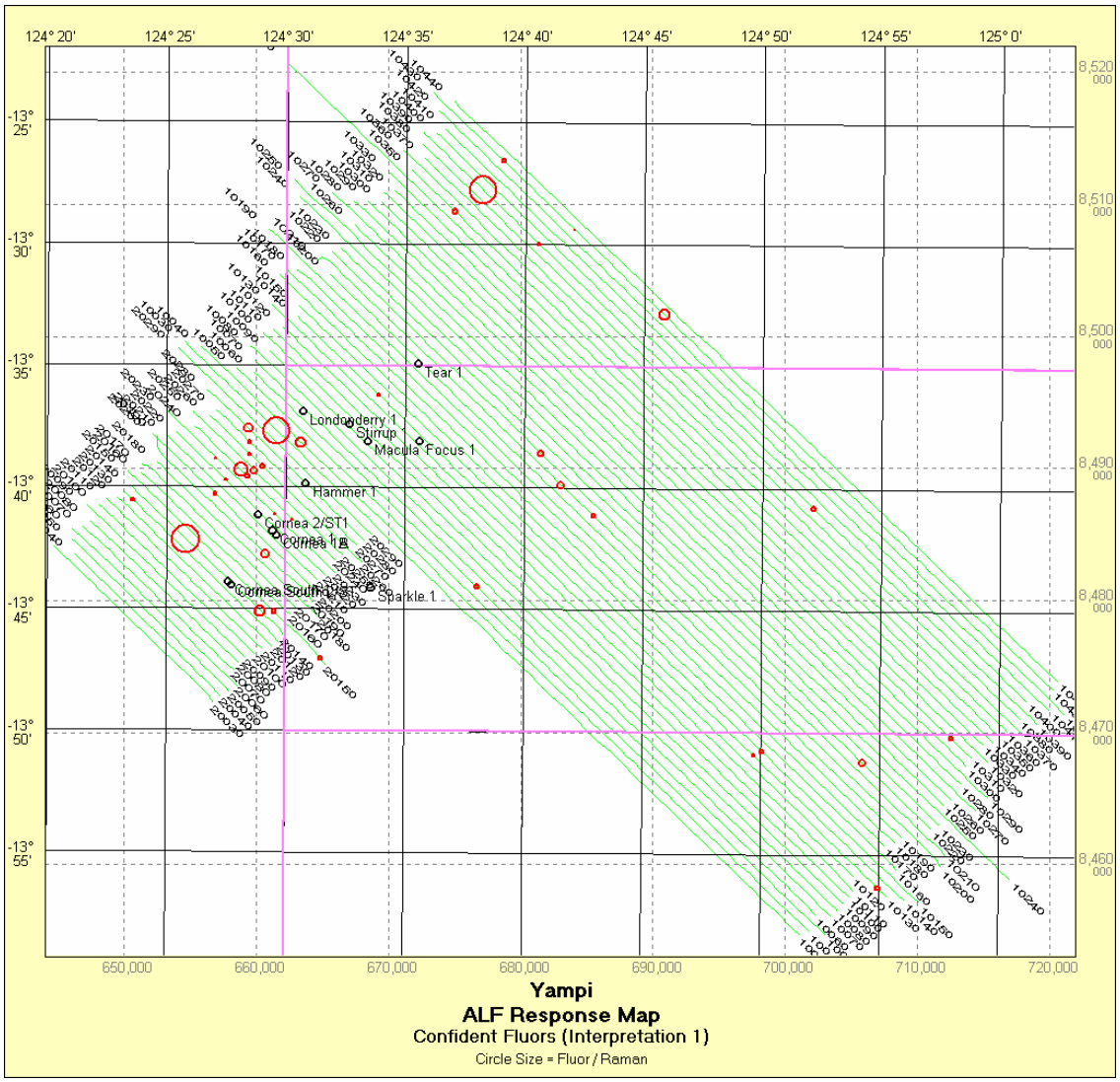

Figure 3. The Yampi ALF Survey Confident Anomaly Map.

2.2. Refined Fluor Mapping

The fluorescence anomaly mapping was refined in a second interpretation. To reduce the effects of acquisition parameters on the initial automatic selection of possible fluors, they were selected using the ratio of channel 50 amplitudes (in the fluorescence region) to channel 27 amplitudes (near the Raman peak).

The following SQL query was used:

SELECT * FROM [RawAlfData] WHERE Ch_50 > Ch_27 / 20 ORDER BY Ch_50 DESC

This reduced the number of possible fluors to 5547. (By sorting on channel 50, the actual fluors tend to be located at the top of the list.)

A more careful interpretation, selecting lower intensity fluors than in the first pass interpretation, resulted in 132 fluors picked. The map of these is shown in Figure 4. Most of the higher intensity fluors are picked in both interpretations but the more detailed interpretation shows a more accurate low intensity fluor distribution.

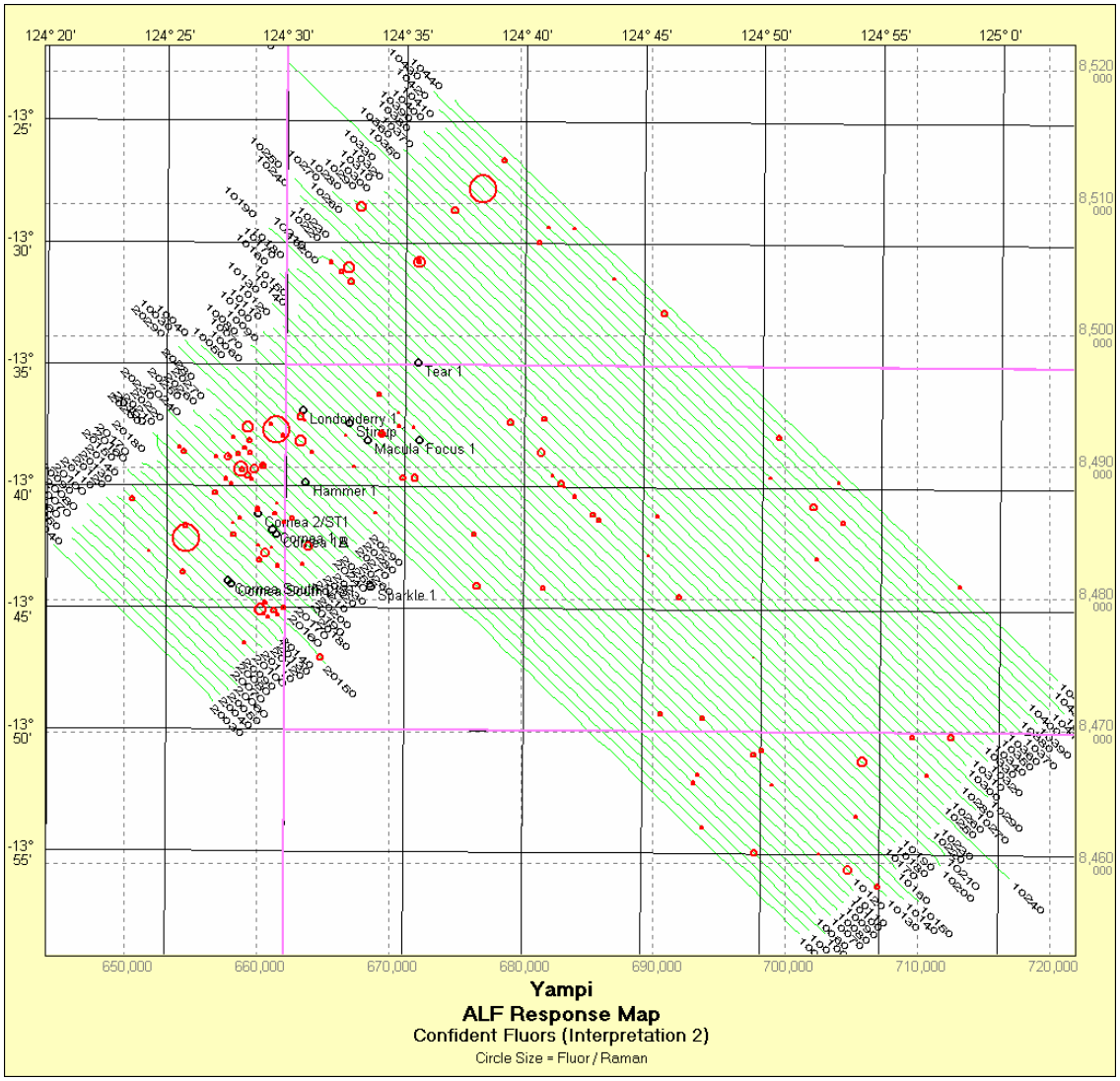

Figure 4. The Yampi ALF Survey Confident Anomaly Map, Interpretation 2.

The fluorescence area / Raman area ratio ranges from 1.43 to 0.14 over the 132 picked fluors. There are many more low ratio (and low intensity) fluors than high ratio fluors. A histogram of the F/R distribution is shown in Figure 5. There are very few fluors in the lowest intensity interval because they are very difficult to pick above the noise in the data. It may be possible in the future to improve the interpretation techniques to reliably detect low intensity fluors.

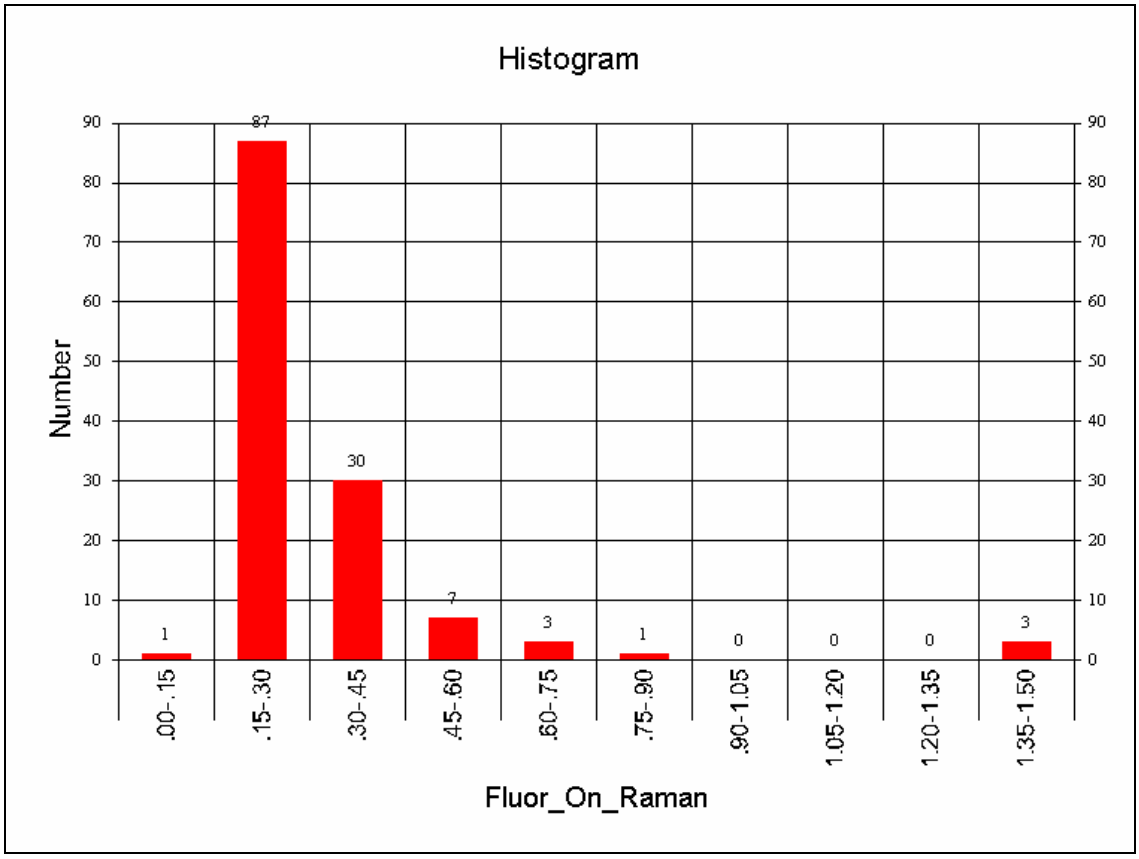

Figure 5. The F/R Ratio Histogram for the Picked Fluors.

Figure 6 on the next page shows a selection of ALF spectra including the smallest and largest fluors picked during the interpretation. Figure 6a is not normalized, while figure 6b to 6f are normalized to the Raman peak.

Line 10220, point 12195 (Figure 6c) has a fluorescence area / Raman area (F/R) ratio of 0.139. Line 10390, point 214241 (Figure 6f) has a F/R ratio of 1.43.

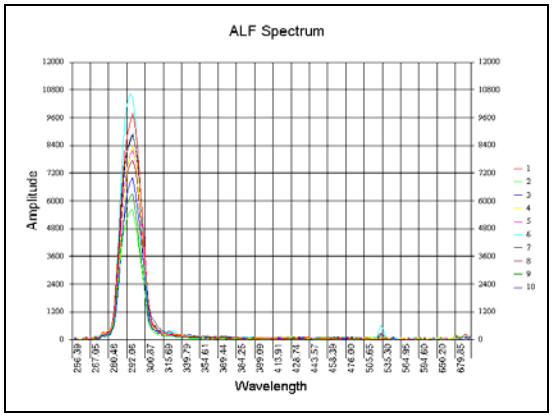

6 a) Line 10030 Ten Adjacent ALF Spectra.

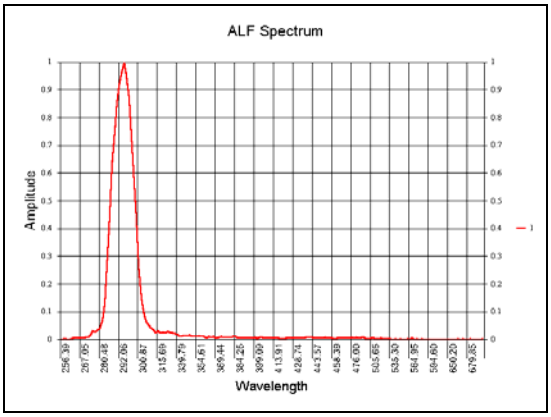

6 b) Line 10030 No Fluor.

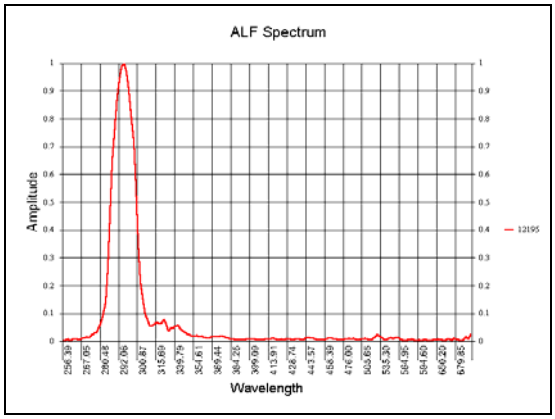

6 c) Line 10220 Low Amplitude Fluor.

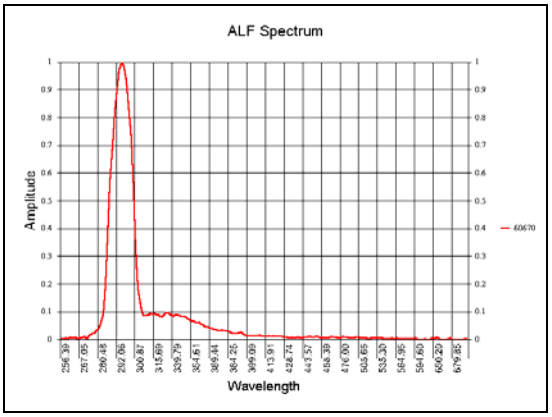

6 d) Line 20230 Medium Amplitude Fluor.

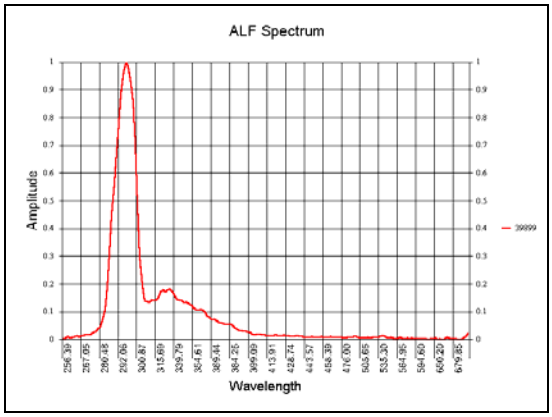

6 e) Line 10350 Medium Amplitude Fluor.

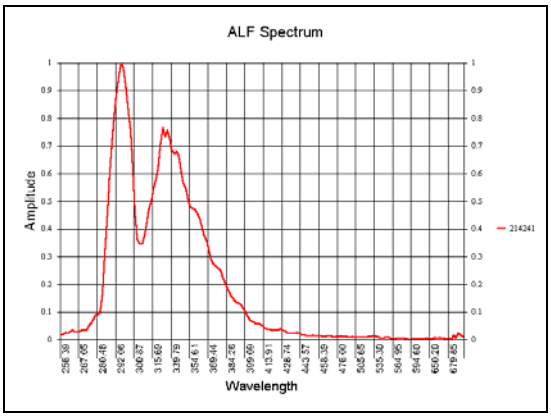

6 f) Line 10390 High Amplitude Fluor.

Figure 6. Selected ALF Spectra.

2.3. Adjacent Fluor Detection

Three adjacent fluors were found on the refined confident anomaly interpretation. They are located on line 10280 at points 323749, 323750 and 323751. These fluors are plotted in Figure 7 below. These curves are plotted without normalisation.

Although the fluorescence curves can be assumed to caused by the same patch of oil, their shapes show some differences. This highlights the difficulties in defining oil type by fluorescence curve shape. This method may be more effective where the noise levels are lower and fluorescence area to Raman area ratios are higher.

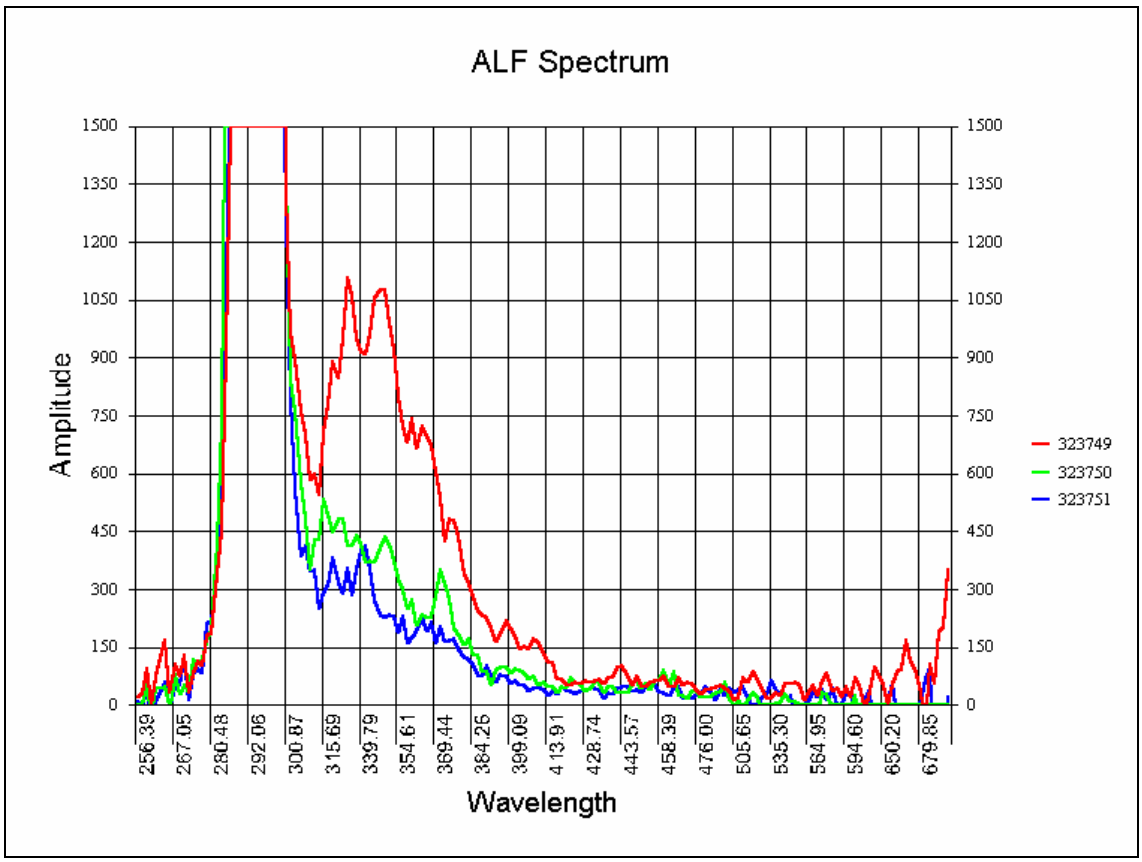

Figure 7. Line 10280 Adjacent Fluors.

There is evidence of the fluorescence response extending between points 323700 and 323754. Figure 8 shows a plot of the 8 fluors that were picked in this interval. These curves are plotted without normalization.

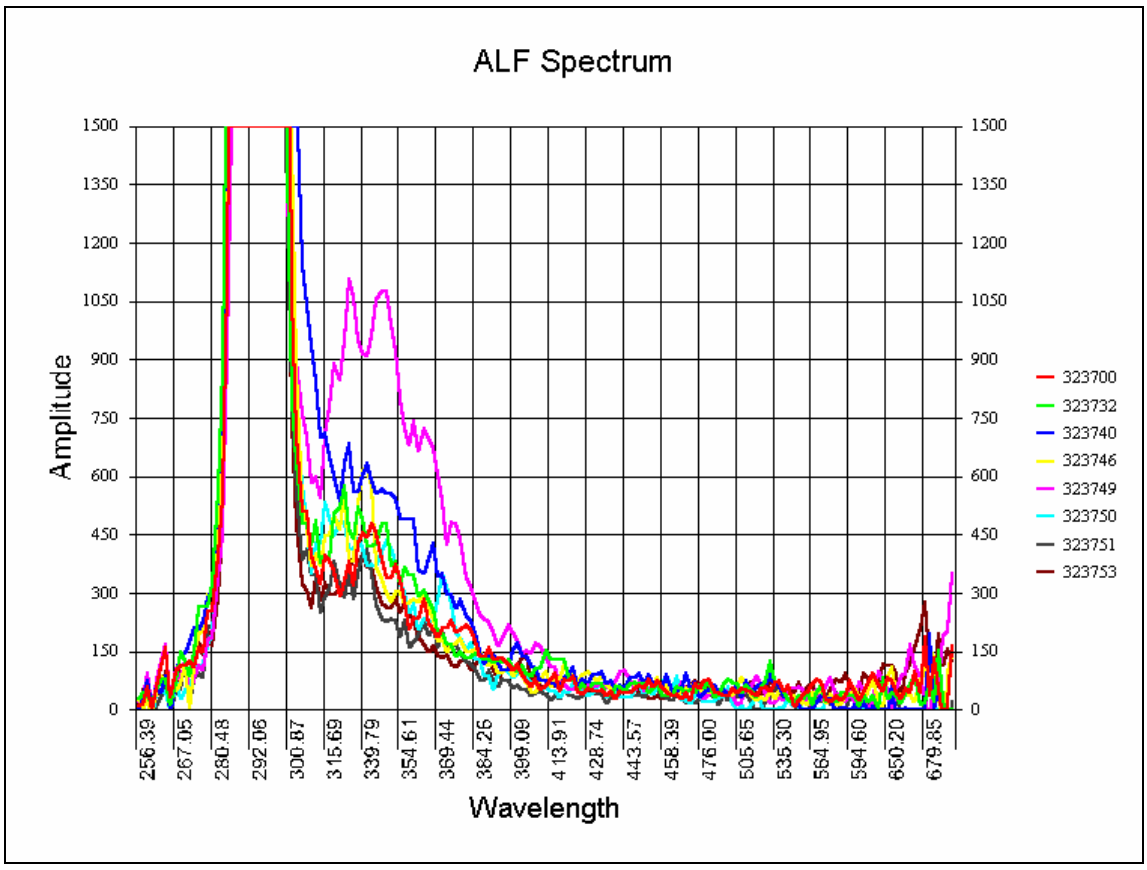

Figure 8. Eight Close Fluors on Line 10280.

The group of fluors is plotted on the map in Figure 9 in blue. These have relatively low ratio of fluorescence area / Raman area and were not picked on the first quick look interpretation.

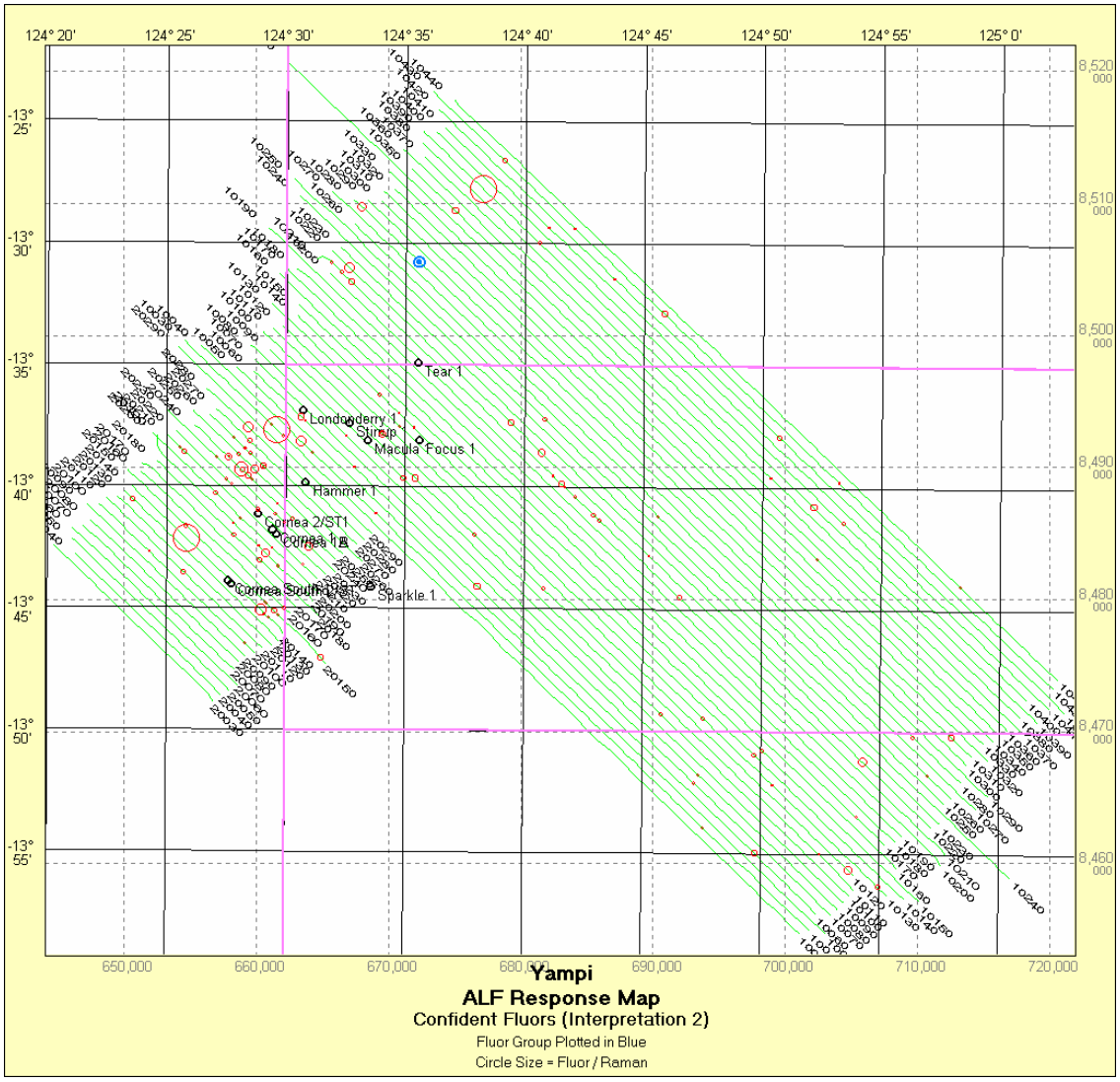

Figure 9. The Yampi ALF Survey Near Fluor Map.

2.4. Fluorescence Curve Trend Analysis

No significant fluorescence response trends were found in the Yampi ALF survey data. Four groups of fluors were identified according to curve shape.

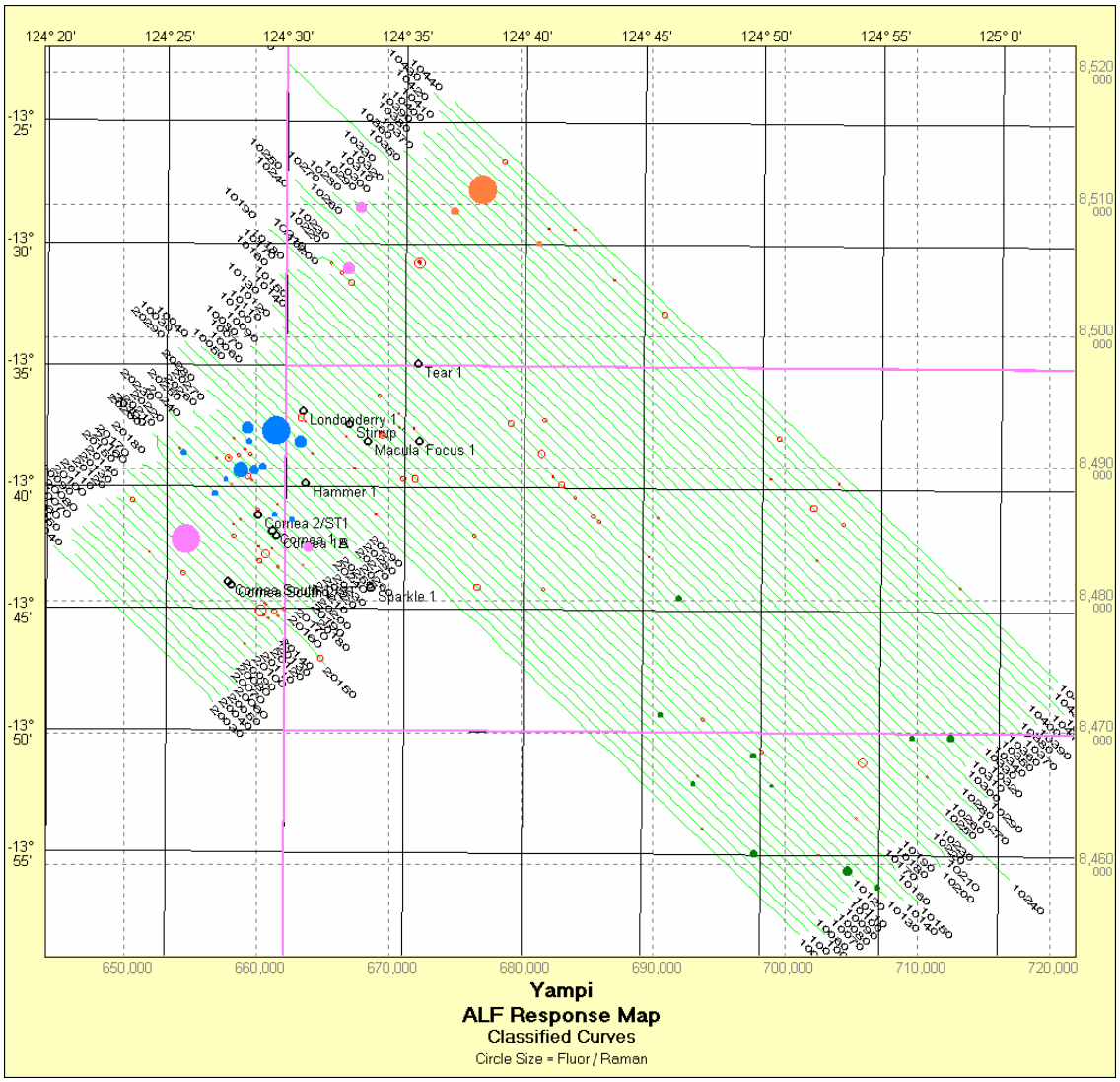

Figure 10. The Yampi ALF Survey Classified Fluor Map.

Group 1 plotted in blue on the fluor map (Figure 10) consist of fluors of similar shape to the SW of the Londonderry-1 well. These fluors are plotted in Figure 11, normalized to the fluorescence peak.

Group 2, plotted in light purple on the fluor map, show fluorescence peaks at particularly long wavelengths. They are not restricted to any one location. These fluors are plotted in Figure 12.

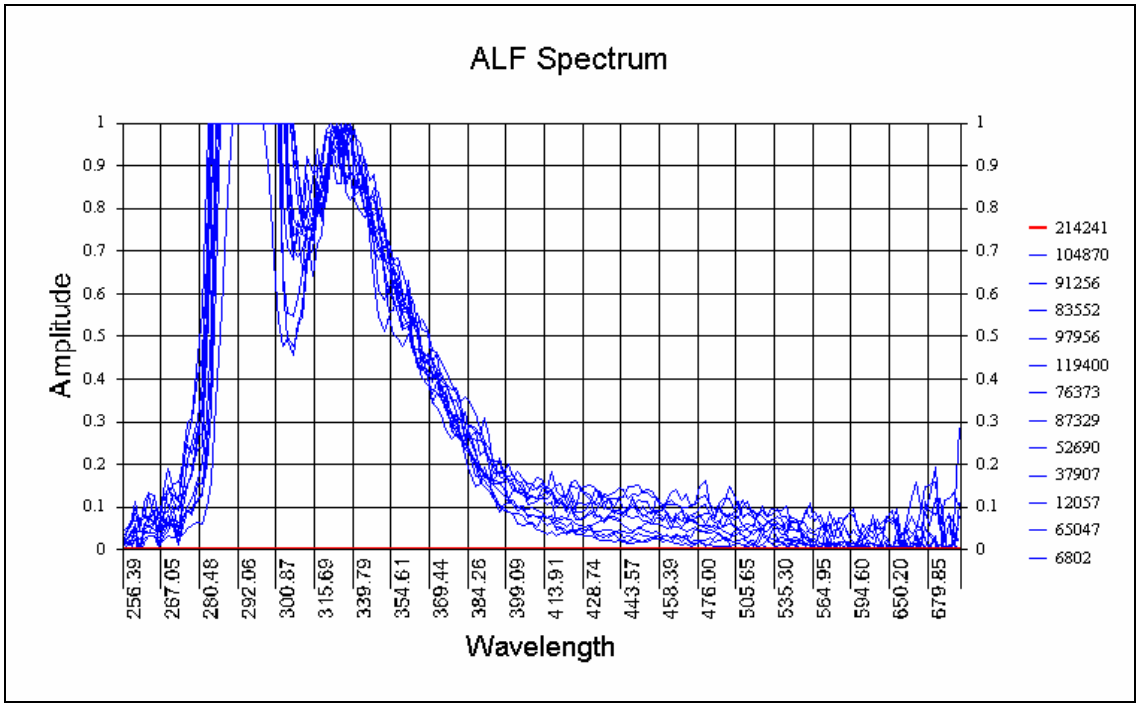

Figure 11. Classified Fluor Group 1.

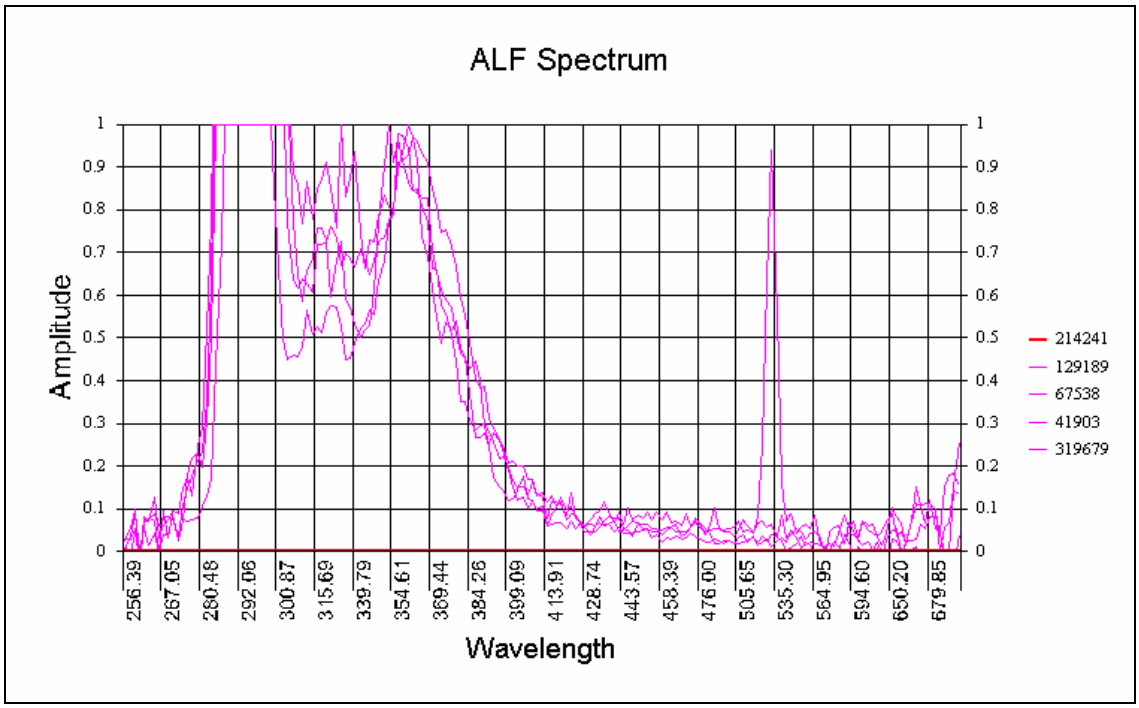

Figure 12. Classified Fluor Group 2.

Group 3, plotted in dark green on the fluor map, consist of fluors of similar shape in the SE part of the survey. They are plotted in Figure 13.

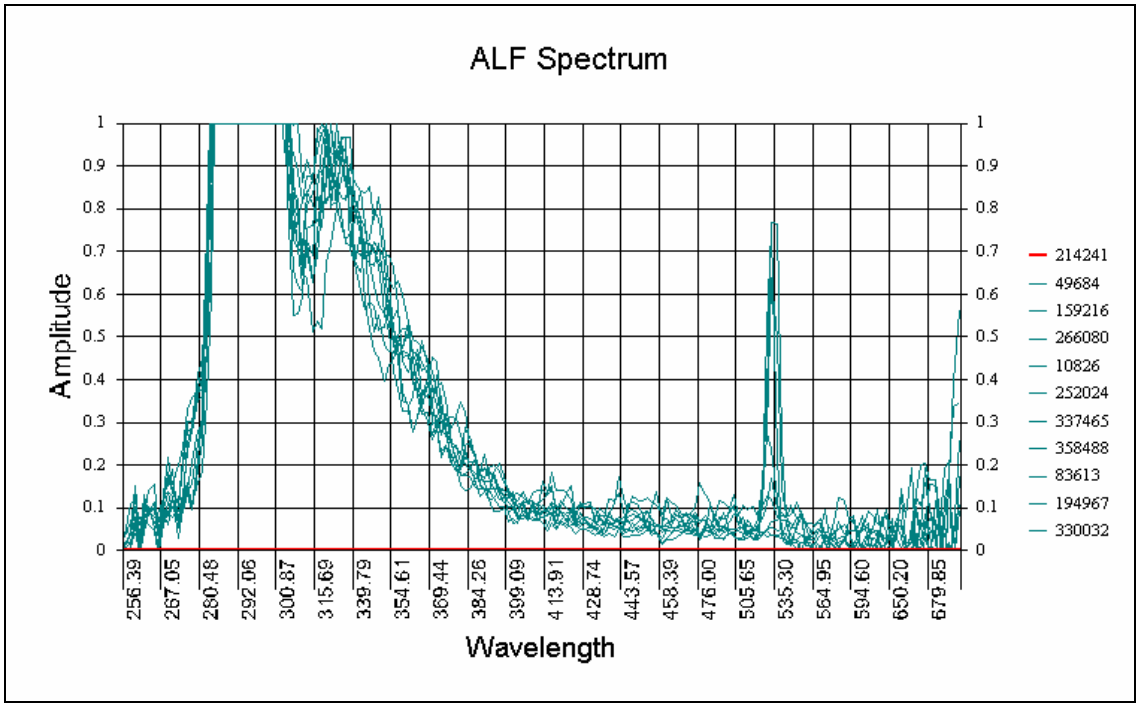

Figure 13. Classified Fluor Group 3.

Group 4, plotted in orange on the fluor map, consist of fluors of similar shape in the northern part of the survey. They are plotted in Figure 14.

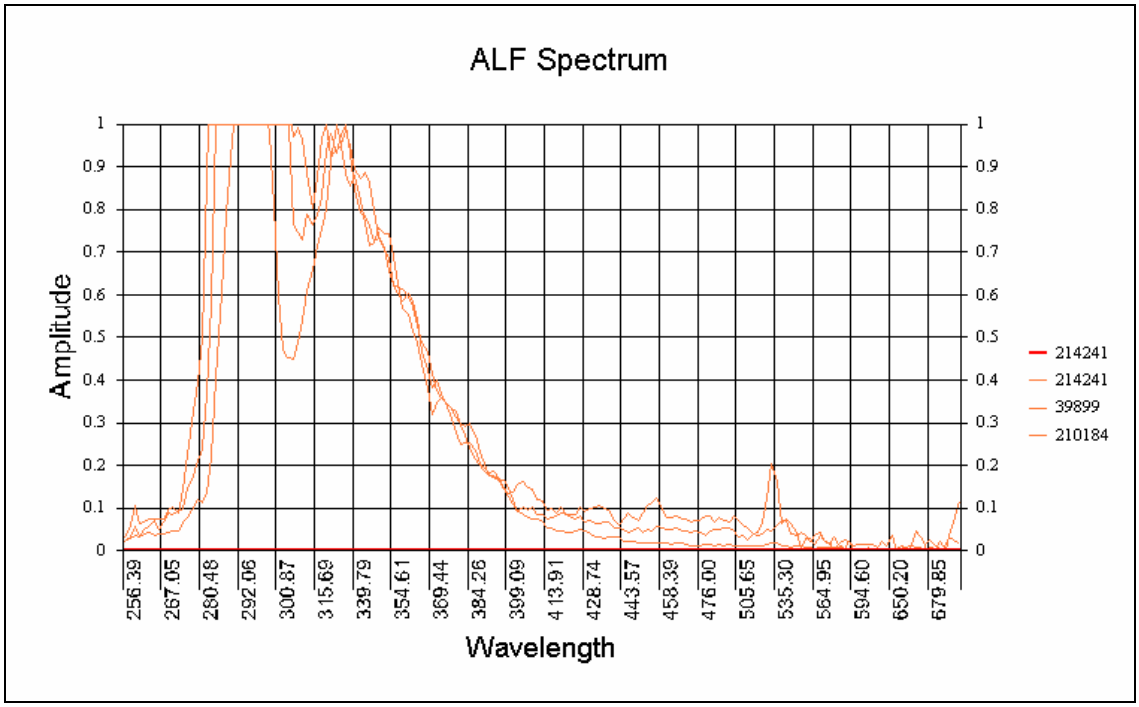

Figure 14. Classified Fluor Group 4.

2.5. Correlation to Seismic Data

Some of the fluorescence anomalies interpreted on the Yampi ALF survey may be related to features seen on seismic data in the area. Figure 15 shows a NW-SE oriented seismic line passing through the Londonderry-1 well. This line shows a shallow hydrocarbon related diagenetic zone (HRDZ) about 1km SE of Londonderry-1 as shallow as 100ms to 150ms below the sea floor. Another deeper HRDZ is seen further to the SE over the NE extension of the Cornea Field.

The shallower HRDZ and fluors near the Londonderry-1 well may relate to present day leakage from a small accumulation. The deeper HRDZ and lack of fluors over the Cornea Field to the SE is consistent with an earlier phase of leakage.

The leakage patterns may also relate to the onlap patterns of sealing units, with leakage occurring at the onlap edges. Geoff O'Brien has presented this model with supporting sniffer, ALF and SAR data.

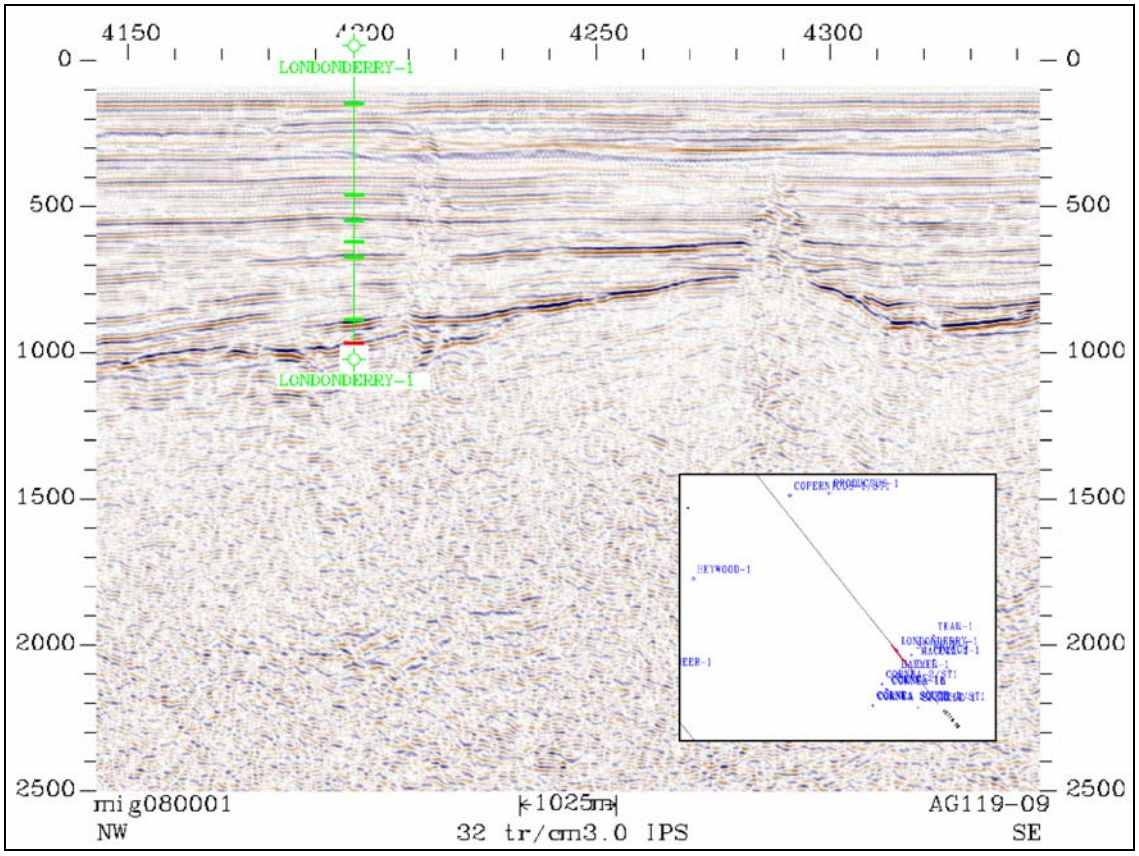

Figure 15. Seismic Line Through Londonderry-1 and the Cornea Field.

3. Conclusions and Recommendations

A detailed interpretation of the Yampi ALF survey shows a main cluster of fluors in the Londonderry-1 and Cornea Field region. This region also contains most of the fluors with the highest fluorescence / Raman area ratios, together with a high density of lower amplitude fluors.

The fluor size histogram shows rapidly increasing numbers of fluors in lower amplitude ranges. The very low number of lowest amplitude fluors picked is caused by the difficulty in confidently identifying them against the background noise. The higher number of low intensity fluors suggests they may provide better areal definition of hydrocarbon leakage. Improved interpretation methods to increase the number of confident low intensity fluors picked may improve the leakage mapping.

A high amplitude fluor and a cluster of lower amplitude fluors are located in the northern part of the survey. The remaining survey area contains a scattering of low amplitude fluors showing no obvious patterns.

No significant trends in fluorescence curve shape were found over the survey area. More work could be done to develop methods to automatically map fluor shape trends.

A cluster of fluors found near the Londonderry-1 well may be related to a shallow HRDZ seen on seismic data in this area. A review of more seismic data in the region would be required to confirm this relationship.

No attempt has been made in this interpretation to identify possible algae fluorescence. World Geoscience Corporation uses video records to identify any algal mats or streaks and associated fluorescence is flagged as possibly due to algae. It may also be possible to identify algae by the fluorescence curve shape.

Appendix 1. Data Acquisition QC

Line	Sections	Clipped	Avg Raman Peak	Avg Raman Variance
10030	452	0	10,788	15,494,620
10040	442	0	11,771	15,332,460
10050	425	0	10,843	16,874,080
10060	384	0	10,544	15,309,350
10070	419	0	7,049	12,441,200
10080	423	0	9,799	15,148,220
10090	423	0	6,541	11,359,790
10100	416	0	7,838	7,816,761
10110	421	0	7,021	14,612,100
10120	406	0	6,826	10,125,700
10130	440	0	8,265	10,268,260
10140	436	0	9,039	4,508,440
10150	449	0	11,767	19,696,660
10160	450	0	10,932	16,716,900
10170	433	0	8,243	3,937,489
10180	434	0	11,567	18,152,220
10190	466	0	11,245	16,661,990
10200	446	0	11,472	16,821,990
10210	451	0	9,258	26,246,440
10220	430	0	11,196	15,005,240
10230	440	0	9,263	10,602,350
10240	517	0	8,497	11,457,620
10250	471	0	9,994	12,823,410
10260	422	0	8,475	13,144,360
10270	454	0	7,975	12,197,140
10280	427	0	8,844	10,578,280
10290	449	0	8,465	11,665,070
10300	424	0	10,771	6,609,542
10310	424	0	8,123	3,984,769
10320	434	0	9,007	4,949,332
10330	426	0	9,291	5,833,061
10340	492	0	9,190	10,225,030
10350	429	0	9,864	14,092,070
10360	440	0	11,443	17,207,000
10370	433	0	8,786	12,949,680
10380	434	0	9,409	15,332,930
10390	444	0	10,414	16,390,710
10400	429	0	11,085	17,708,720
10410	429	0	9,055	15,857,320
10420	461	0	8,668	21,030,970

Table 1a. Yampi ALF Survey Data Acquisition Summary.

Line	Sections	Clipped	Avg Raman Peak	Avg Raman Variance
10430	435	0	8,776	16,832,380
10440	426	0	8,834	14,267,130
20030	111	0	11,464	16,833,130
20040	103	0	9,973	12,349,510
20050	110	0	9,712	11,585,380
20060	119	0	10,978	14,190,630
20070	108	0	13,091	15,644,140
20080	107	0	12,460	20,387,180
20090	114	0	9,540	13,203,570
20100	110	0	10,936	16,490,600
20110	111	0	9,915	14,201,980
20120	110	0	11,203	16,357,500
20130	109	0	11,490	19,311,990
20140	108	0	11,605	20,373,460
20150	141	0	10,629	17,331,180
20160	106	0	12,670	22,123,340
20170	108	0	12,337	21,220,140
20180	106	0	10,523	12,333,670
20190	119	0	10,816	20,425,420
20200	115	0	11,345	16,370,070
20210	113	0	9,993	16,576,410
20220	111	0	12,075	18,141,880
20230	124	0	10,821	17,337,190
20240	102	0	11,389	17,456,150
20250	109	0	10,538	15,426,240
20260	106	0	10,711	15,698,330
20270	97	0	10,605	16,368,930
20280	109	0	9,954	18,145,710
20290	143	0	10,771	13,630,560

Table 1b. Yampi ALF Survey Data Acquisition Summary (cont).

The data acquisition curves showed the average Raman peak at acceptable ranges for all lines. There were some sudden changes in the level indicating the parameters were changed during acquisition. The averaged Raman variance showed some regions of high magnitude. In some cases this corresponded to acquisition problems such as on line 10210.

Many types of noise were observed on records in this survey including random noise, high glint amplitudes usually with spurious fluorescence peaks, large long wavelength amplitude trend, clipping and zeroed values.

The acquisition QC curve for line 10210 is shown in Figure 16. Some of the increases in Raman peak and variance correspond to noisy record zones. The line starts to have very noisy records from point 220372. This problem continues to the end of the line at point 220782. Figure 17 shows an example of a noisy record from this line. A similar noise problem is seen on line 10060 (eg point 71813), but in this case it affects only occasional isolated records.

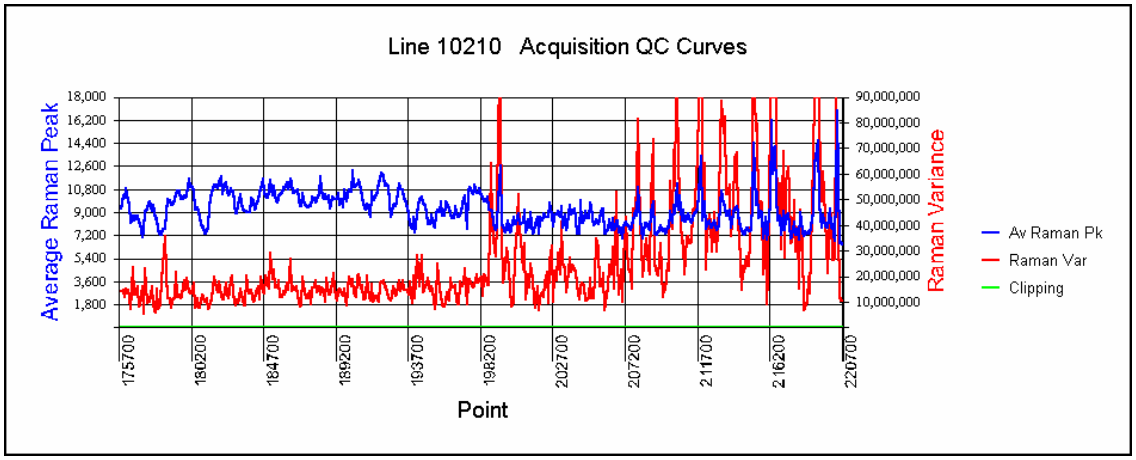

Figure 16. Line 10210 Acquisition QC Curves.

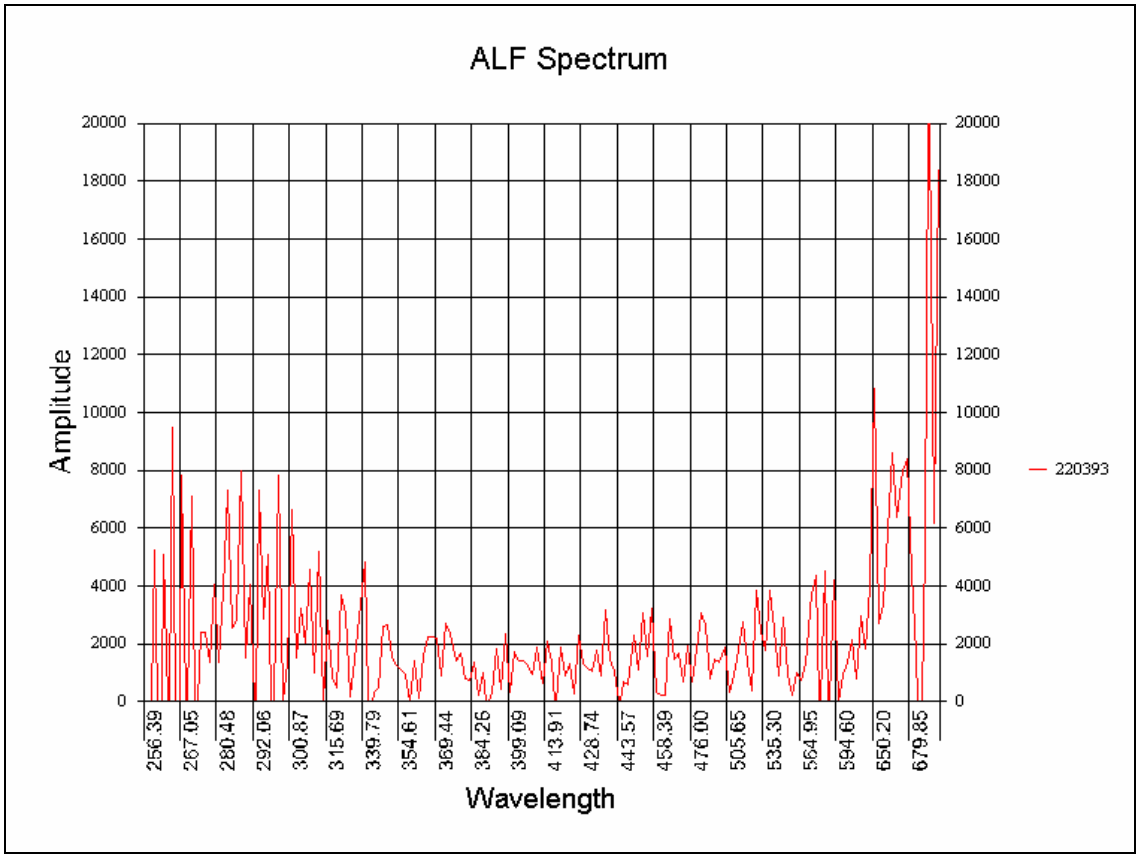

Figure 17. Line 10210 Noisy Record Example.

Noisy records are occasionally seen with very large glint response and peaks within the fluorescence region of the spectrum. An example of this noise is shown on line 10410, point 39026 (Figure 18). It is also seen on line 10210, point 211346, line 10410, point 16817, line 10410, point 17161, line 10440, point 43555, line 10340, point 1514. A large response may also be seen near the excitation wavelength (eg line 10430, point 137954).

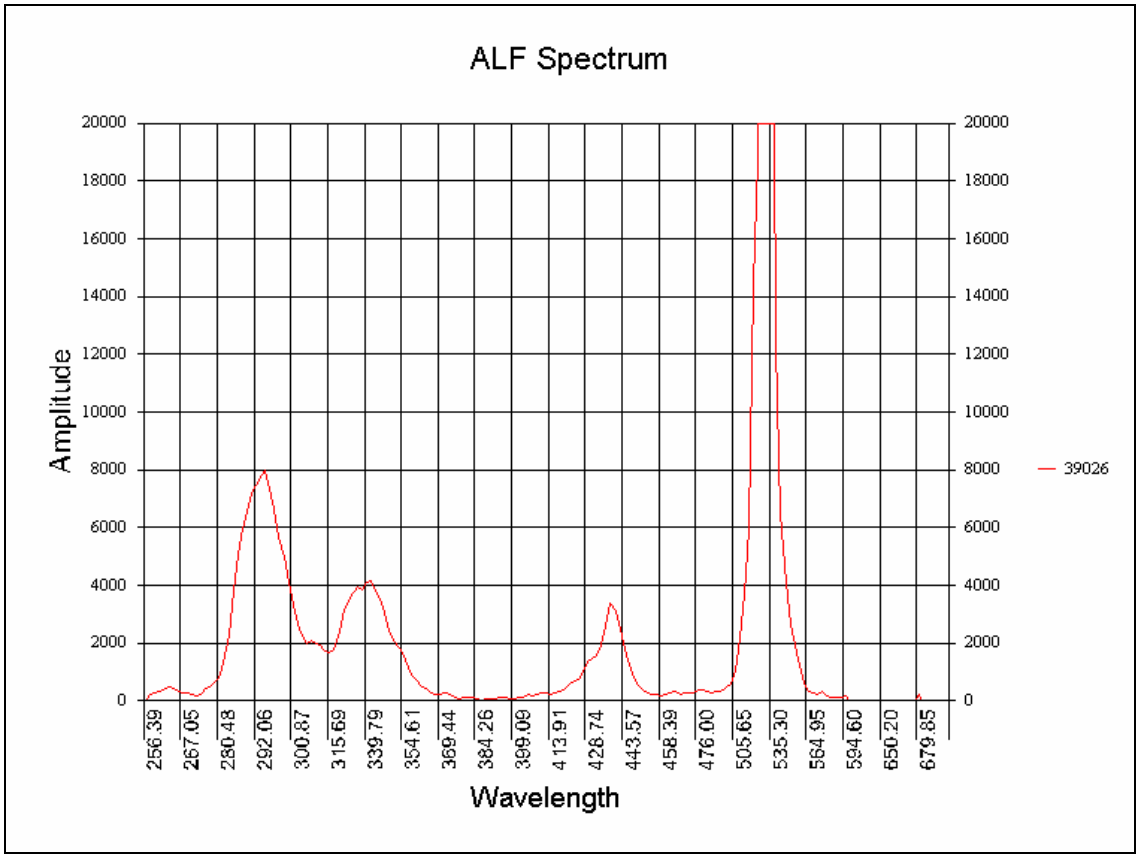

Figure 18. Line 10410 Noisy Record Example.

Line 20030 shows a record at point 4327 with very high amplitudes on the long wavelengths (Figure 19). This type of noise is only seen rarely. Other examples are seen on line 10280, point 350991 and line 10050, point 6141. This noise may be caused by sunglint.

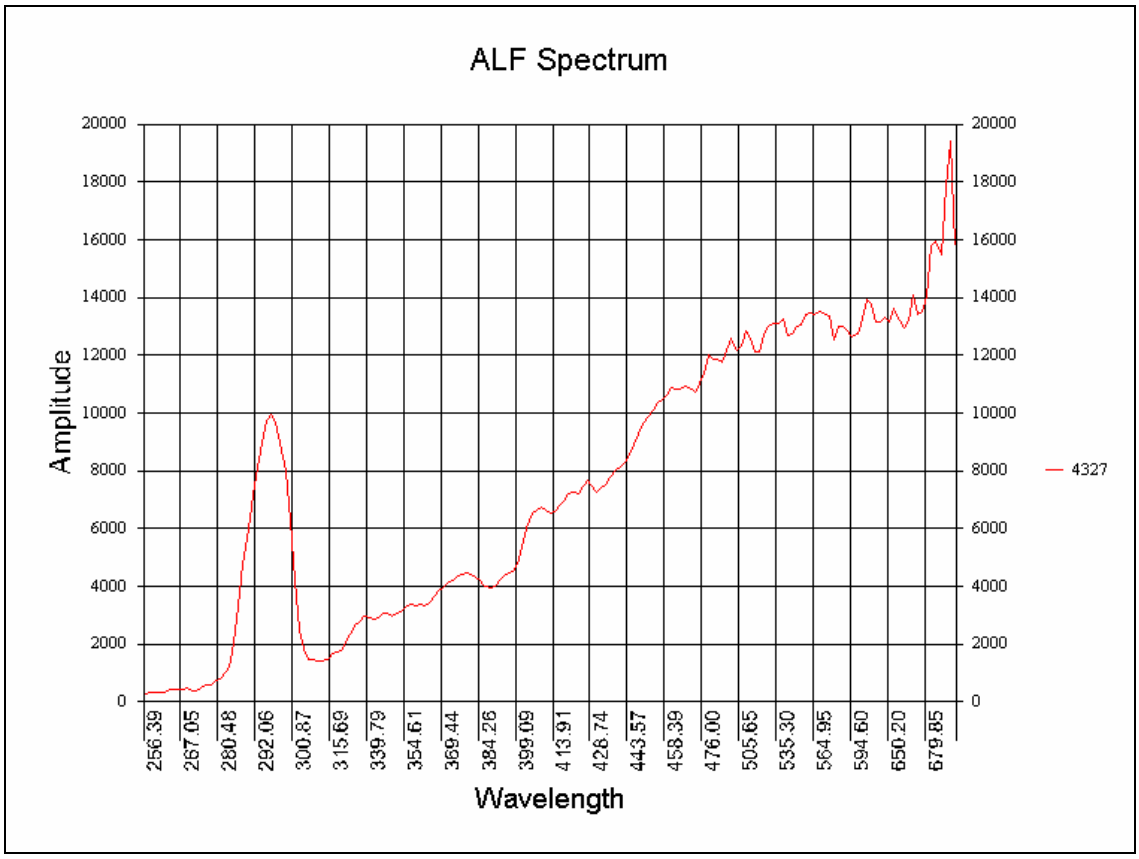

Figure 19. Line 20030 Noisy Record Example.

Some clipped records were noted during the data interpretation. Figure 20 shows the record on line 10420, point 95250 with a clipped Raman peak. The data appears to have been rescaled so clipping cannot be detected by checking peak amplitudes. Line 10160, point 100288 shows another example of data clipping.

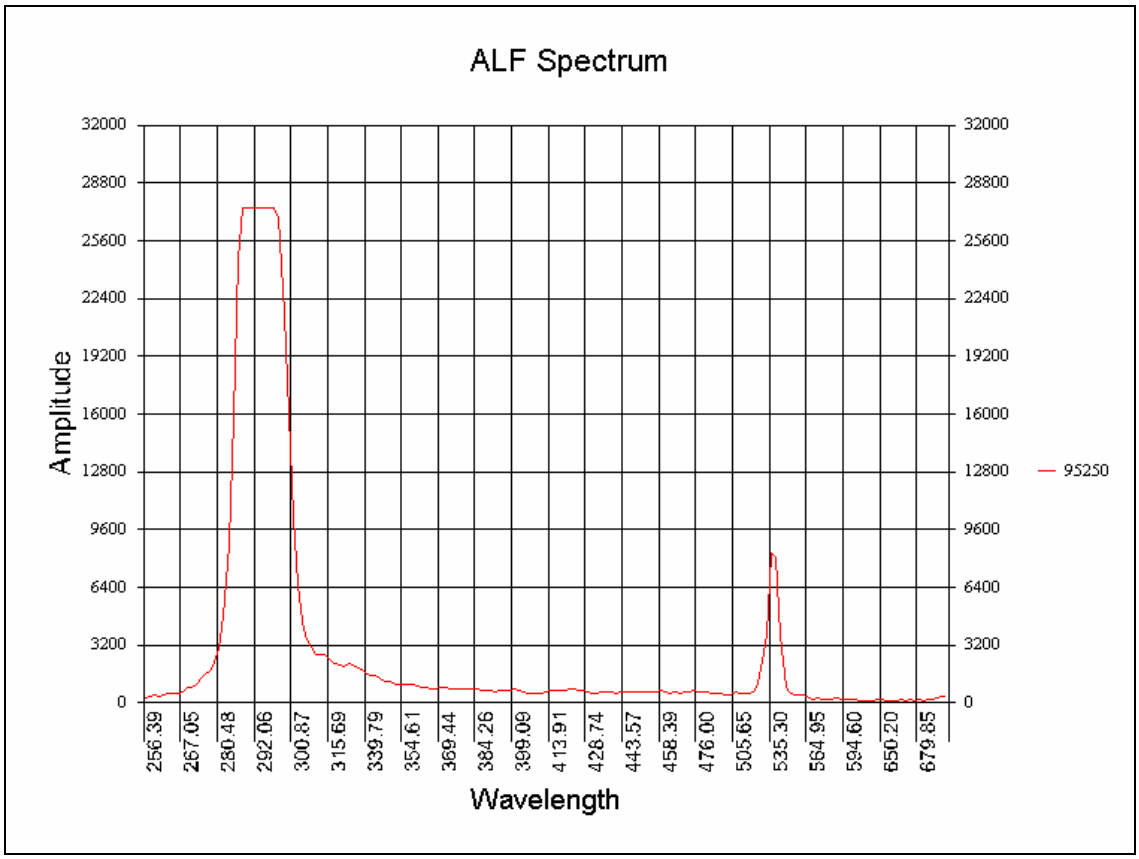

Figure 20. Line 10420 Clipped Record.

Line 10360, points 46527 (Figure 21) shows a record with zero amplitude on the long wavelengths. This type of distortion is seen occasionally. Other examples are seen on line 20240, point 85193 and line 10440, point 47231.

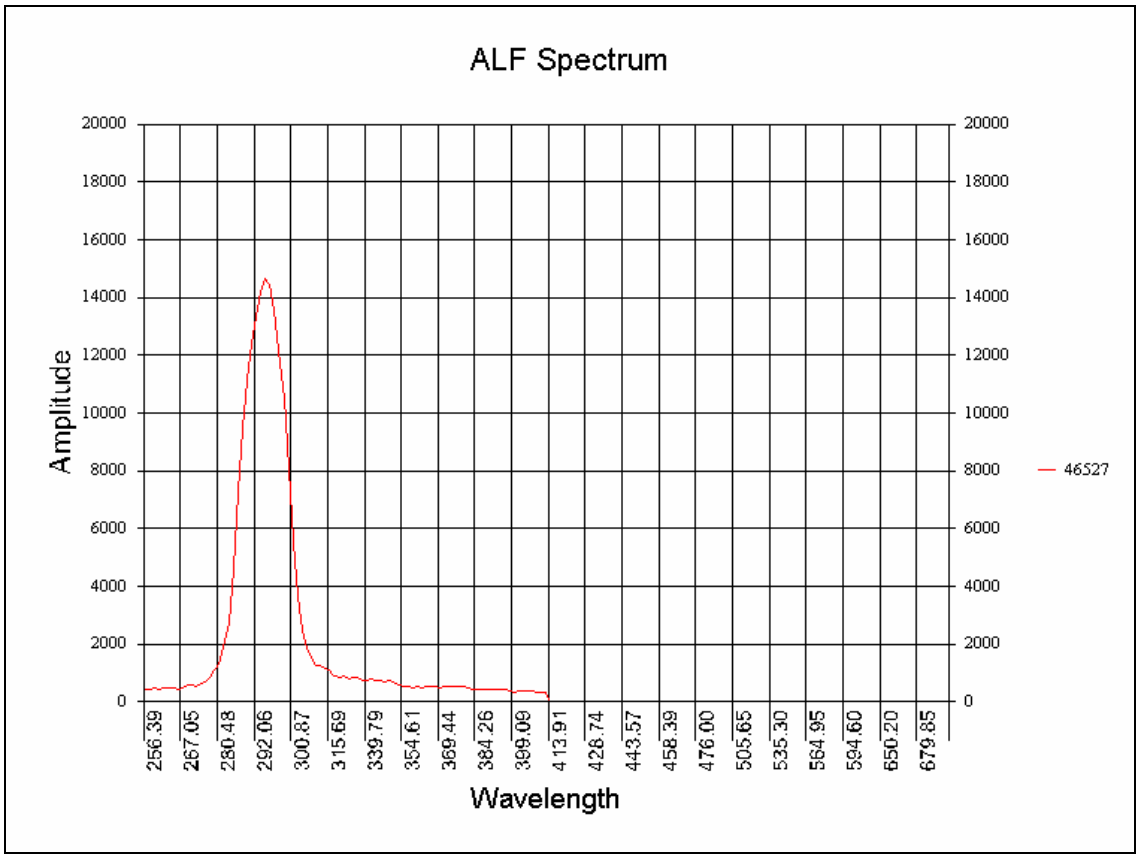

Figure 21. Line 10360 with Zero Amplitudes at Long Wavelengths.

Line 10420, point 113719 (Figure 22) is an example of a record having a very large glint amplitude.

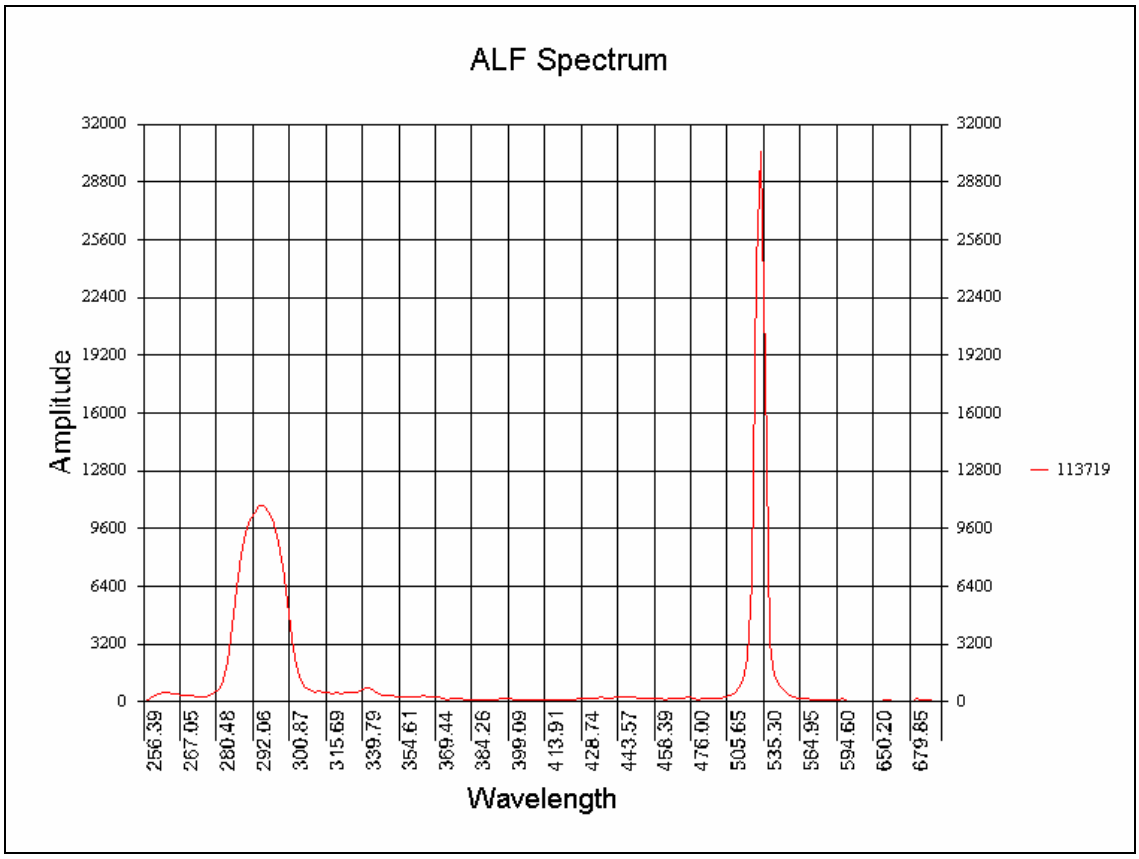

Figure 22. Line 10420 Large Glint Example.

Line 20210 suffers from low amplitude records and noise bursts from point 11253 to point 11695. This can be seen as anomalous values on the acquisition QC curves that can be viewed using the ALF Tools software.

Appendix 2. Data Navigation QC

Line	Heading (deg)	Straight Line Distance (m)	Acquisition Time (seconds)	Avg Straight Line Velocity (km/hr)	Points	Flight Distance (m)	Avg Flying Velocity (km/hr)	Avg Point Spacing (m)
10030	134.06	64,651.35	895.49	259.91	45,379	64,697.40	260.09	1.43
10040	133.96	63,892.79	874.47	263.03	44,289	63,910.16	263.10	1.44
10050	314.00	61,884.52	841.97	264.60	42,643	61,886.94	264.61	1.45
10060	314.10	59,127.00	760.47	279.90	38,514	59,134.71	279.94	1.54
10070	134.02	60,619.29	828.98	263.25	41,985	60,624.29	263.27	1.44
10080	133.94	61,679.21	836.98	265.29	42,390	61,690.30	265.34	1.46
10090	314.00	60,348.29	836.48	259.72	42,365	60,352.50	259.74	1.42
10100	313.99	61,564.23	823.50	269.13	41,706	61,566.46	269.14	1.48
10110	314.14	61,206.08	833.00	264.52	42,238	61,217.69	264.57	1.45
10120	133.99	59,974.67	803.99	268.55	40,719	59,977.86	268.56	1.47
10130	133.99	64,658.41	869.97	267.56	44,060	64,662.43	267.58	1.47
10140	313.96	63,721.50	862.98	265.82	43,707	63,727.60	265.85	1.46
10150	313.97	65,138.77	889.48	263.64	45,049	65,142.90	263.65	1.45
10160	314.02	64,878.33	890.98	262.14	45,125	64,882.28	262.16	1.44
10170	134.09	62,794.73	857.99	263.48	43,454	62,811.70	263.55	1.45
10180	133.87	62,774.41	857.98	263.40	43,454	62,788.68	263.46	1.45
10190	133.92	66,460.20	923.48	259.08	46,771	66,468.75	259.11	1.42
10200	314.22	64,464.16	882.47	262.98	44,694	64,528.41	263.24	1.44
10210	313.65	65,599.02	892.48	264.61	45,200	65,841.77	265.59	1.46
10220	314.02	63,011.39	852.48	266.10	43,174	63,022.50	266.14	1.46
10230	313.99	62,992.86	869.98	260.67	44,059	63,000.98	260.70	1.43
10240	313.96	74,575.16	1,023.98	262.18	51,859	74,586.92	262.22	1.44
10250	133.99	68,256.45	931.48	263.80	47,174	68,291.81	263.94	1.45
10260	134.01	62,774.77	835.47	270.49	42,314	62,779.43	270.51	1.48
10270	133.90	67,594.75	898.49	270.83	45,503	67,603.13	270.87	1.49
10280	133.94	63,711.21	843.97	271.76	42,744	63,717.15	271.79	1.49
10290	313.98	65,227.23	888.49	264.29	44,998	65,234.02	264.32	1.45
10300	314.01	61,520.92	840.96	263.36	42,592	61,523.68	263.37	1.44
10310	134.00	61,730.86	837.49	265.35	42,411	61,735.07	265.37	1.46
10320	314.00	62,429.80	859.49	261.49	43,552	62,432.98	261.50	1.43
10330	133.98	62,594.43	843.97	267.00	42,743	62,597.97	267.02	1.46
10340	133.99	74,236.05	973.48	274.53	49,303	74,251.35	274.59	1.51
10350	314.01	61,835.59	849.97	261.90	43,047	61,839.18	261.92	1.44
10360	134.00	63,484.70	871.47	262.25	44,136	63,489.80	262.27	1.44
10370	314.02	62,942.77	856.98	264.41	43,403	62,947.70	264.43	1.45
10380	134.00	62,831.67	858.48	263.48	43,478	62,835.99	263.50	1.45
10390	314.00	64,571.44	877.99	264.76	44,467	64,575.38	264.78	1.45
10400	134.00	62,090.86	847.59	263.72	42,976	62,097.71	263.75	1.45
10410	313.99	63,565.20	850.98	268.91	43,099	63,573.36	268.94	1.48
10420	314.08	65,822.89	911.97	259.84	46,186	65,834.52	259.88	1.43

Table 2a. Line Navigation Summary.

Line	Heading (deg)	Straight Line Distance (m)	Acquisition Time (seconds)	Avg Straight Line Velocity (km/hr)	Points	Flight Distance (m)	Avg Flying Velocity (km/hr)	Avg Point Spacing (m)
10430	134.02	65,242.55	861.97	272.48	43,655	65,255.40	272.54	1.49
10440	133.96	63,446.05	841.97	271.28	42,643	63,472.47	271.39	1.49
20030	314.63	16,957.67	221.97	275.03	11,241	16,993.95	275.62	1.51
20040	314.22	15,387.31	204.98	270.24	10,382	15,390.25	270.29	1.48
20050	314.19	16,546.64	219.00	272.00	11,092	16,549.69	272.05	1.49
20060	133.71	17,273.88	237.47	261.87	12,028	17,286.49	262.06	1.44
20070	133.70	15,784.28	214.98	264.32	10,889	15,787.06	264.37	1.45
20080	133.70	15,575.90	213.98	262.05	10,838	15,577.61	262.08	1.44
20090	134.00	16,664.81	225.99	265.47	11,445	16,666.17	265.49	1.46
20100	133.72	16,335.93	219.98	267.34	11,140	16,345.05	267.49	1.47
20110	314.13	16,465.59	220.99	268.23	11,193	16,467.13	268.26	1.47
20120	313.97	16,263.00	219.49	266.74	11,117	16,266.02	266.79	1.46
20130	314.29	16,346.96	217.47	270.61	11,015	16,362.99	270.87	1.49
20140	314.60	16,086.58	215.48	268.76	10,914	16,142.48	269.69	1.48
20150	314.48	20,963.15	279.50	270.01	14,207	20,982.21	270.25	1.48
20160	133.63	15,633.85	210.49	267.39	10,661	15,642.32	267.53	1.47
20170	132.91	15,880.36	214.99	265.92	10,889	15,950.25	267.09	1.47
20180	313.97	16,920.22	212.46	286.70	10,760	16,923.40	286.76	1.57
20190	316.80	17,263.45	236.49	262.79	11,977	17,528.66	266.83	1.46
20200	314.13	17,580.06	229.97	275.20	11,648	17,584.83	275.28	1.51
20210	133.93	15,721.67	224.48	252.13	11,368	15,722.68	252.15	1.38
20220	134.01	15,696.60	220.81	255.91	11,235	15,701.40	255.99	1.40
20230	134.05	17,682.23	245.98	258.78	12,459	17,694.58	258.97	1.42
20240	133.56	14,727.28	203.47	260.57	10,306	14,745.21	260.89	1.43
20250	134.13	15,748.75	217.48	260.69	11,015	15,752.61	260.76	1.43
20260	314.17	16,069.31	210.48	274.85	10,661	16,070.71	274.87	1.51
20270	314.20	14,820.77	194.49	274.33	9,851	14,824.83	274.41	1.51
20280	313.87	16,521.33	215.49	276.01	10,965	16,550.27	276.49	1.51
20290	134.06	20,387.33	285.99	256.63	14,483	20,388.50	256.65	1.41
Total		**3,129,231.47**	**42,426.59**		**2,149,037**	**3,130,508.68**		

Table 2b. Line Navigation Summary (cont).

Tables 2a and 2b summarise the navigation performance for the Yampi ALF survey. A more detailed assessment can be made by using the ALF Tools software to review the navigation QC curves.

Navigation parameters were acceptable but a variation in flight speed was noticed for many of the lines. Average flight speed ranged from 256km/hr to 280km/hr.

Most lines were flown within 10m of the nominal altitude and within 100m of a straight flight path.

Figure 23 shows the navigation QC curves for line 10330. While the average flight speed was 267 km/hr, the speed ranged from 250 to 280 km/hr. The black inline deviation curve shows that some points were displaced by over 600m from the location they would be if the line was flown at a constant speed.

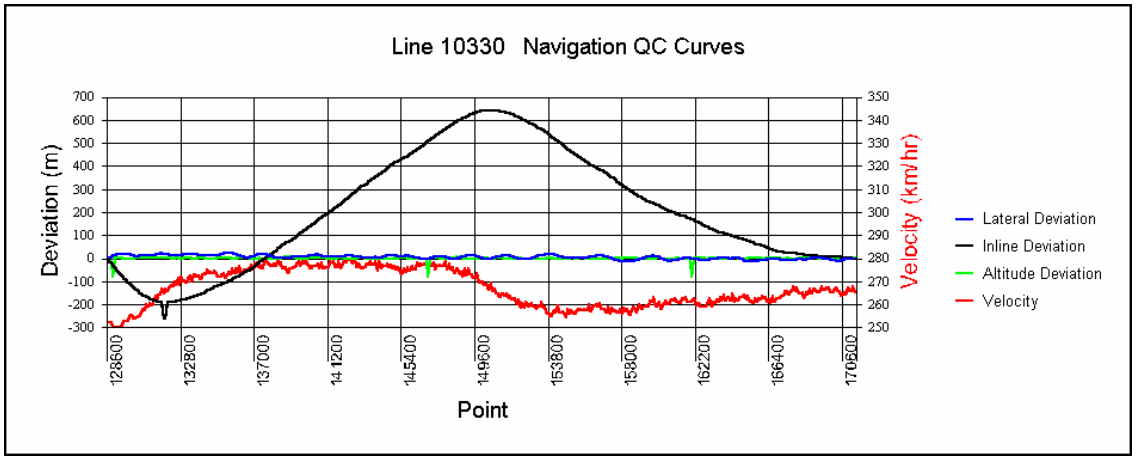

Figure 23. Line 10330 Navigation QC Curves.

Appendix 3. CD Contents

A CD containing ALF analysis data is included in the back of this report.
The CD contains the following files:

ALF Power.map
ALF Explorer map definition file for the ALF power map.

ALFAnalysis.dat
ALF Explorer project data file. (This file together with the Acp16.mdb file forms the ALF Explorer project data.)

Confident Anomalies Interp1.dat
ASCII data file of the first pass confident fluors picked during the interpretation.

Confident Anomalies Interp2.dat
ASCII data file of the final confident fluors picked during the interpretation.

Fluor Peak Wavelen.map
ALF Explorer map definition file for the fluor peak wavelength map.

Fluors and ALF Power.map
ALF Explorer map definition file for the fluor and ALF power map.

Line 10280 Eight Adjacent Fluors.dat
ASCII data file of eight adjacent fluors picked on line 10280.

Line 10280 Three Adjacent Fluors.dat
ASCII data file of three adjacent fluors picked on line 10280.

Prelim Interp ALF Response.map
ALF Explorer map definition file for the first pass fluor map.

Refined Interp ALF Response.map
ALF Explorer map definition file for the final fluor map.

Survey Map.map
ALF Explorer map definition file for the ALF survey map.

Yampi ALF Survey Interp Report.doc
The Yampi ALF survey interpretation report.

Yampi Survey Summary.xls
Survey summary spreadsheet.

Yampi.mdb
ALF Explorer project database containing interpretation results.

Figures
Directory containing figures used in the interpretation report.